Mercury Adsorption Properties of Sulfur-Impregnated Adsorbents

Hsing-Cheng Hsi[1]; Mark J. Rood, M.ASCE[2]; Massoud Rostam-Abadi[3]; Shiaoguo Chen[4]; and Ramsay Chang[5]

Abstract: Carbonaceous and noncarbonaceous adsorbents were impregnated with elemental sulfur to evaluate the chemical and physical properties of the adsorbents and their equilibrium mercury adsorption capacities. Simulated coal combustion flue gas conditions were used to determine the equilibrium adsorption capacities for Hg^0 and $HgCl_2$ gases to better understand how to remove mercury from gas streams generated by coal-fired utility power plants. Sulfur was deposited onto the adsorbents by monolayer surface deposition or volume pore filling. Sulfur impregnation increased the total sulfur content and decreased the total and micropore surface areas and pore volumes for all of the adsorbents tested. Adsorbents with sufficient amounts of active adsorption sites and sufficient microporous structure had mercury adsorption capacities up to 4,509 μg Hg/g adsorbent. Elemental sulfur, organic sulfur, and sulfate were formed on the adsorbents during sulfur impregnation. Correlations were established with $R^2 > 0.92$ between the equilibrium $Hg^0/HgCl_2$ adsorption capacities and the mass concentrations of elemental and organic sulfur. This result indicates that elemental and organic sulfur are important active adsorption sites for Hg^0 and $HgCl_2$.

DOI: 10.1061/(ASCE)0733-9372(2002)128:11(1080)

CE Database keywords: Mercury; Adsorption; Combustion; Activated carbon; Fly ash; Zeolite; Sulfur.

Introduction

Carbon-based adsorption processes (e.g., direct injection and fixed bed) have the potential to remove elemental and oxidized mercury species at very low concentrations (e.g., $\approx \mu g/m^3$ levels) that exist in flue gas streams generated during the combustion of coal (Chang and Offen 1995). It has also been established that activated-carbon adsorbents can be developed with larger mercury (Hg^0 and $HgCl_2$) adsorption capacities by impregnating the samples with sulfur (Steijns et al. 1976; Krishnan et al. 1994; Livengood et al. 1994; Korpiel and Vidic 1997; Liu et al. 1998; Hsi et al. 2001). Recent studies have provided a better understanding of the effects of impregnated sulfur on the chemical and physical properties of activated carbon and the resulting mercury adsorption capacities of the samples (Hsi et al. 1998, 2001). Impregnating activated carbons with elemental sulfur at 250–650°C resulted in an increase in the total sulfur content and a decrease in the total surface area and micropore (pores widths ≤20 Å) surface area of activated carbon samples when compared to the untreated samples (Korpiel and Vidic 1997; Liu et al. 1998; Hsi et al. 1998, 2001).

Sulfur impregnation at 250°C into activated carbon fibers (ACFs); (0 wt % sulfur, 1,886 m^2/g micropore surface area, and 350 μg/g equilibrium Hg^0 adsorption capacity) resulted in the largest total sulfur content (64 wt %), an undetectable micropore surface area, and the smallest equilibrium Hg^0 adsorption capacity (755 μg/g) for treated samples in a simulated flue gas stream containing 50 $\mu g/m^3$ Hg^0 at 140°C (Hsi et al. 2001). Notably, sulfur impregnation at 400°C increased the ACF sample's total sulfur content to 44 wt %, decreased the micropore surface area to 81 m^2/g, and resulted in the largest equilibrium Hg^0 adsorption capacity (11,343 μg/g). Sulfur impregnation at 650°C increased the sulfur content of the ACFs to ~13 wt %, caused a 12% reduction in micropore surface area, and increased the equilibrium Hg^0 adsorption capacity for the sample to 1,907 μg/g. Such adsorption capacity is comparable to those of activated carbons derived from high organic-sulfur content coals (908–2,947 μg/g) (Hsi et al. 1998, 2001).

Results described above indicate that the total amount of sulfur in activated carbons or the sample's total surface area do not necessarily determine the samples' mercury adsorption capacities independently. Sulfur *K*-edge x-ray absorption near-edge structure (S-XANES) spectroscopy examinations and CS_2 extraction tests on sulfur-impregnated ACFs suggest that sulfur in its elemental forms provides one of the most active sites for Hg^0 adsorption

[1]Assistant Professor, Dept. of Safety, Health, and Environmental Engineering, National Kaohsiung First University of Science and Technology, Kaohsiung, Taiwan, R.O.C.; formerly, PhD, Dept. of Civil and Environmental Engineering, Univ. of Illinois at Urbana-Champaign, 205 N. Mathews Ave., Urbana, IL 61801.

[2]Professor, Dept. of Civil and Environmental Engineering, Univ. of Illinois at Urbana-Champaign, 205 N. Mathews Ave., Urbana, IL 61801 (corresponding author). E-mail: mrood@uiuc.edu

[3]Adjunct Associate Professor, Dept. of Civil and Environmental Engineering, Univ. of Illinois at Urbana-Champaign, 205 N. Mathews Ave., Urbana, IL 61801; formerly, Head and Senior Chemical Engineer, Energy and Environmental Engineering, Illinois State Geological Survey, 615 E. Peabody Dr., Champaign, IL 61820 (corresponding author). E-mail: masoud@isgs.uiuc.edu

[4]Chemical Engineer, Illinois State Geological Survey, 615 E. Peabody Dr., Champaign, IL 61820.

[5]Manager, Particulate and Air Toxics Control, Energy Conversion Division, EPRI, 3412 Hillview Ave., Palo Alto, CA 20036.

Note. Associate Editor: Wendell P. Ela. Discussion open until April 1, 2003. Separate discussions must be submitted for individual papers. To extend the closing date by one month, a written request must be filed with the ASCE Managing Editor. The manuscript for this paper was submitted for review and possible publication on August 24, 2001; approved on February 13, 2002. This paper is part of the ***Journal of Environmental Engineering***, Vol. 128, No. 11, November 1, 2002. ©ASCE, ISSN 0733-9372/2002/11-1080–1089/$8.00+$.50 per page.

(Hsi et al. 2001). Pore size distributions of the same samples indicate that the micropores in ACFs are also needed to achieve the large Hg^0 adsorption capacities. It appears that it is the combination of active sulfur sites and the appropriate porous structure in activated carbons that results in large Hg^0 adsorption capacities. However, the influence of active sulfur forms and the micropore surface area of the adsorbents in capturing mercury (i.e., Hg^0 and $HgCl_2$) in coal-combustion flue gases are still not well understood.

Cost is an important issue in adsorbent-based processes for removing mercury from flue gases generated during the combustion of coal. Current estimates predict very high costs associated with mercury control, with activated carbon costs representing a large fraction of the overall costs (United States Environmental Protection Agency) (USEPA 1997). In order to make adsorbent injection for mercury removal more feasible, it is necessary to either reduce the amount of adsorbent needed, or decrease the cost of adsorbent production. Sulfur impregnation of ACFs at 400°C appears optimal for the development of a high Hg^0 adsorption capacity activated carbon. However, the cost for raw ACFs used in our studies is \$300–1,000/kg (American Kynol, Inc., Pleasantville, N.Y. personal communication). It would be useful to evaluate other low-cost or unique adsorbents that are impregnated with sulfur at similar conditions as described above to better understand the factors that most influence the samples' mercury adsorption capacities. It would also be useful to determine if there are better low-cost materials available that can be used to remove mercury from coal-combustion flue gas streams.

In this study, several carbonaceous and noncarbonaceous adsorbents were impregnated with elemental sulfur between 300 and 400°C to evaluate their resulting chemical/physical properties and equilibrium $Hg^0/HgCl_2$ adsorption capacities. These carbonaceous adsorbents are fly ash, coal-derived activated carbons (CDACs), pistachio shell char (PSC), and pistachio activated carbon (PAC). The noncarbonaceous adsorbents are zeolites. These samples have a wide range in cost, with some of them available as recovered industrial or agricultural byproducts. The influence of sulfur impregnation at 300–400°C on the properties and equilibrium Hg^0 and $HgCl_2$ adsorption capacities of these samples were then examined and compared to results obtained from the ACF samples (Hsi et al. 2001).

Research Methodology and Instrumentation

Preparation of Raw Adsorbents

Fly Ash and Coal-Derived Activated Carbon

Fly ash is a byproduct generated by the electric utility industry that is low cost. It typically has a small total surface area (N_2 Brunauer, Emmett, and Teller, BET) no detectable micropore surface area, low carbon content, and contains 70–90% of the particles as glassy spheres (Adriano et al. 1980). Fly ash samples were obtained from the Abbott Power Plant, Univ. of Illinois (Champaign, Ill.). The high sulfur (4.0 wt %) Illinois bituminous coal used to produce the fly ash samples was burned by one of Abbott's15 MW_e stoker-fired boilers. This high sulfur coal has been used to produce several CDACs (Hsi et al. 1998). Results obtained from fly ash samples are categorized with the coal-based carbonaceous adsorbents because they originated from coal and contain ash with small amounts of carbon. Fly ash produced from burning the same coal in a pulverized coal-fired unit may not be the same as reported here.

Coal-derived activated carbons have already been shown to have relatively high Hg^0 and $HgCl_2$ adsorption capacities (Krishnan et al. 1994; Korpiel and Vidic 1997; Hsi et al. 1998; Liu et al. 1998). Coal-derived activated carbons were either produced in a pilot-scale fluidized-bed reactor or obtained commercially. PILOT-5 samples (Table 1) were produced from a high-sulfur (4.1 wt %) Illinois bituminous coal using a pilot-scale fluidized-bed reactor (Hsi et al. 1998). This coal and the fly ash described above came from the same coal mine. The commercially available CDACs studied here are lignite-based Darco FGD from Norit Americas Inc. (Atlanta) and bituminous-based FG3 from Waterlink Sutcliffe Carbons (Lancashire, U.K.).

Pistachio Shell Char and Pistachio Activated Carbon

Pistachio shells are low cost agricultural byproducts. Pistachio shell char was prepared by initially crushing the shells to 5–10 mm in width and then feeding the sample at rate of ~50 kg/h into an indirectly fired pilot-scale rotary kiln (3.4 m long with a 45 cm i.d.). Samples were carbonized in a N_2 environment for 30 min at 675°C in the kiln. Pistachio activated carbon was prepared in a bench-scale reactor. In a typical run about 5 g of ~5-mm wide shells were placed in a ceramic boat; the boat was inserted inside a 5 cm i.d. ceramic reactor tube and then heated by a tubular furnace (Lindberg, Model 59344). The sample was simultaneously carbonized and activated with steam (50% H_2O/50% N_2; gas flow rate=1 L/min at standard temperature and pressure) at 800°C for 30 min in the furnace.

Zeolite

Unlike most activated carbons, which have slit-like pores with polydisperse size distributions, zeolites A (NaA) and Y (CBV-400) have cylindrical pores that are monodisperse. The kinetic diameters of pores are 3.5/3.9 and 8.1 Å, respectively (Breck 1973). These noncarbonaceous samples were obtained to evaluate the effectiveness of monodisperse aluminosilicate adsorbents for mercury adsorption, and compare their mercury adsorption capacities to those for the carbonaceous adsorbents. Zeolite A (SiO_2/Al_2O_3 molar ratio=1) was provided by the Dept. of Material Science and Engineering, Univ. of Illinois (Urbana, Ill.). The sample was synthesized in a bench-scale aluminosilicate–gel hydrothermal system (Kerr 1966; Breck 1973). The Zeolite Y sample (SiO_2/Al_2O_3 molar ratio=5.1) was obtained commercially (Zeolyst International Inc., Valley Forge, Pa.)

Sulfur Impregnation

Typically, CDAC, PAC, and zeolite samples of 2 g were physically mixed with elemental sulfur (1:1 sulfur to adsorbent mass ratio) in a ceramic boat (7.5 cm long, 2 cm wide) and then heated in the tubular furnace at 400°C for 6 h (Lindberg, Model 59344). Ultrahigh purity (UHP) N_2 continuously flowed (<50 mL/min) through the furnace to maintain an oxygen-free environment. After thermal treatment, the samples were cooled for 24 h to room temperature with UHP N_2 passing through the furnace tube. The cooled samples were then ground in a CO_2 environment (Spec Agate Laboratory mill/grinder) for 10–15 min in preparation for sample characterization and mercury adsorption tests. The resulting samples were designated X-S400, where X represents the type of raw sample and S400 represents the sample's sulfur-impregnation temperature (Table 1).

Sulfur-impregnated fly ash and PSC samples were produced by physically mixing the samples with 0.02 or 0.05 elemental sulfur to sample mass ratio. Fly ash samples were treated at

Table 1. Physical Properties, Chemical Properties and Equilibrium Mercury Adsorption Capacities of Raw and Sulfur-Impregnated Samples (Fly Ash, Coal Derived Activated Carbon, Pistachio Shell Char, Pistachio Activated Carbon, Zeolite, and Activated Carbon Filter)

Precursor	Sample code	Sulfur content (wt %)	Total surface area (m^2/g)	Micropore surface area (m^2/g)	Mesopore surface area (m^2/g)	Total pore volume (cm^3/g)	Micropore volume (cm^3/g)	Hg^0 adsorption capacity[a] ($\mu g/g$)	$HgCl_2$ adsorption capacity[a] ($\mu g/g$)
Coal fly ash	Raw fly ash	0.1	1.5	ND[b]	NA[c]	0.001	ND	0	4
(Illinois C-3)	FA-S300-2	1.3	0.6	ND	NA	0.001	ND	23	104
	FA-S300-5	4.7	0.5	ND	NA	0.001	ND	38	72
Coal	PILOT-5	1.2	695	563	132	0.391	0.261	617	739
(Bituminous	PILOT5-S400	21.3	160	72	88	0.121	0.034	1,444	3,299
and lignite)	FGD	1.0	503	229	274	0.635	0.105	572	974
	FGD-S400	9.4	328	148	180	0.490	0.069	393	1,447
	FG3	0.0	1,405	463	942	1.169	0.229	259	126
	FG3-S400	22.4	787	282	504	0.621	0.129	1,062	1,056
	Raw shell	0.2	NA	NA	NA	NA	NA	NA	NA
	PSC	0.1	386	361	25	0.208	0.175	341	174
Biomass	PSC-S400-2	2.1	350	326	24	0.196	0.158	492	479
(Pistachio)	PSC-S400-5	3.6	267	249	18	0.152	0.121	308	645
	PAC	0.0	774	672	102	0.505	0.312	383	374
	PAC-S400	17.3	452	351	101	0.330	0.164	908	2,030
	A	0.0	—[d]	—	—	—	—	162	0
Zeolite	A-S400	11.9	—	—	—	—	—	89	NA
	Y	0.0	533	488	45	0.356	0.326	5	2
	Y-S400	17.0	146	112	34	0.087	0.060	133	236
Phenolic	ACF-20	0.0	1,971	1,886	85	0.949	0.872	356	756
Polymer	ACF-20-S400	44.0	94	81	13	0.052	0.037	3,260	4,509

[a]Samples were tested in eastern bituminous coal condition except for FG3, FG3-S400, ACF-20, and ACF-20-S400 that were tested in western subbituminous coal condition.

[b]ND=not detectable.

[c]NA=not available.

[d]N_2 adsorption isotherms were not obtained for zeolite A samples because pore width of samples was smaller than N_2 molecules.

300°C for 1 h instead of 400°C because the elemental sulfur was not retained on the ash at the higher temperature. The PSC samples were treated at 400°C for 1 h. The final products are designated X–SY–Z to describe the type of raw sample, sulfur impregnation temperature, and amount of sulfur used to treat the adsorbent, respectively (e.g., PSC-S400-5 represents the raw PSC samples impregnated with sulfur at 400°C with a 0.05 mass ratio of sulfur to PSC).

Physical and Chemical Characterization of Raw and Sulfur-Impregnated Adsorbents

The total surface area, micropore surface area, and pore size distribution of raw and sulfur-impregnated samples, except for zeolite A, were determined with N_2 adsorption at 77 K (Micromeritics, Model ASAP2400). Samples were degassed at 7.5×10^{-8} to 15×10^{-8} Pa vacuum at 110°C for 24 h before the N_2 adsorption measurements occurred between 10^{-3} and 101,300 Pa. Total surface areas were calculated by the BET equation based on ASTM D4820-96a (ASTM 1997a). Micropore surface areas and volumes were calculated from *t*-plot analyses using the Jura–Harkins equation (Lippens et al. 1964). The range of relative pressures used to determine micropore surface areas and volumes were based on thickness *t* values between 4.5 and 8.0 Å.

Micropore size distributions were determined by the three-dimensional (3D) model (Sun et al. 1998). Mesopore (pores widths between 20 and 500 Å) size distributions were determined by the Barret–Joyner–Halenda method (Gregg and Sing 1967). All of the tested samples had pore widths less than 500 Å resulting in no macropore (pores widths $\geqslant$500 Å) surface areas and volumes. Total sulfur analyses are based on ASTM D4239-94 (ASTM 1997a) using a LECO SC-32 system with a detection range of 0.005–99.99% sulfur. The percent mass of sulfur added to the samples due to sulfur impregnation was defined as the percent mass of sulfur added divided by the mass of resulting product, which can be described as

$$S_{add}\ (wt\,\%) = \frac{S_f - S_i}{1 - S_i} \times 100$$

where S_{add}=increase in the percent mass of sulfur due to sulfur impregnation and is referred to as "sulfur added"; S_i=sulfur mass fraction of the raw sample; and S_f=sulfur mass fraction of the resulting sulfur-impregnated sample.

Selected raw and sulfur-impregnated samples were also examined by S-XANES spectroscopy and x-ray diffraction to determine the forms of sulfur functional groups and to identify the presence of any crystalline elemental sulfur, respectively (Huggins et al. 1993; Hsi et al. 2001).

Mercury Adsorption Capacity Characterization

Raw and sulfur-impregnated samples were stored in air and shipped to URS Corp. (Austin, Tex.) for bench-scale, fixed-bed mercury adsorption tests. A brief description of the test is provided here for clarity (Carey et al. 1998). Tests were carried out using simulated coal-combustion flue gas conditions with a mercury (Hg^0 or $HgCl_2$) concentration of 50 ± 20 $\mu g/N\,m^3$ at 163°C. The flue gases contained O_2(6 vol %), CO_2 (12 vol %), H_2O (7 vol %), select concentrations of HCl, SO_2, and NO_x, and balance N_2. Typically, mercury adsorption tests occurred using the eastern bituminous coal flue gas condition with 50 ppmv HCl, 1,600 ppmv SO_2, and 400 ppmv NO_x. Select samples were tested using the western subbituminous coal flue gas condition with 2 ppmv HCl, 400 ppmv SO_2, and 200 ppmv NO_x. The gas stream passed through a temperature-controlled fixed-bed column (1.3 cm i.d.) containing a 20 mg sample mixed with 10 g sand. The superficial gas velocity through an empty column was about 15 m/min at 24°C. The effluent gas from the fixed-bed column flowed through heated lines to an impinger containing $SnCl_{2(aq)}$ that reduced any oxidized mercury compounds to Hg^0. The gas then flowed through a buffer solution ($Na_2CO_{3(aq)}$) to remove the SO_2 and HCl from the gas. Gas exiting the impinger solutions flowed through a gold amalgamation column housed in a tubular furnace where the mercury in the gas was adsorbed (<100°C). The mercury that was concentrated on the gold was then thermally desorbed (>750°C) and sent as a concentrated mercury stream to a cold-vapor atomic absorption spectrophotometer for analysis.

Equilibrium mercury adsorption capacities (μg Hg adsorbed/g adsorbent) were determined by summing the mass of mercury removed from the gas stream based on the acquired breakthrough curves and then dividing by the mass of the adsorbent in the adsorption bed:

$$\frac{m_i}{m_{\text{adsorbent}}}=\sum_{t=0}^{t'}\frac{(C_{i,\text{in}}-C_{i,\text{out}})\times Q_g}{m_{\text{adsorbent}}}\Delta t$$

where m_i=mass of adsorbed Hg^0 or $HgCl_2$; $m_{\text{adsorbent}}$=total mass of adsorbent; t'=equilibrium breakthrough time; $C_{i,\text{in}}$=experimental inlet Hg^0 or $HgCl_2$ concentration; $C_{i,\text{out}}$=experimental outlet Hg^0 or $HgCl_2$ concentration at time t; Q_g=total gas flow rate; and Δt=experimental time interval. In order to achieve a direct comparison between adsorbents, the measured adsorption capacities were normalized, first by multiplying by 50 $\mu g/N\,m^3$ and then by dividing by the actual inlet concentration. The $HgCl_2$ adsorption capacities were further normalized to exclude the mass of adsorbed chlorine by multiplying by 0.74, which is the ratio of the molecule weights for Hg and $HgCl_2$.

Quality control measurements were performed at the laboratory of URS Corp. to verify proper operation of the bench-scale mercury adsorption tests (Carey et al. 1998). Blanks and quality control samples consisting of gas-phase injections of known mercury ''spikes'' must be within 10% to pass an initial accuracy check. Blank tests conducted with no carbon sample in the sand bed consistently indicated no mercury adsorption. During operation of the test unit, all efforts were made to ensure consistent operation of all test parameters. However, some inconsistencies periodically occurred because the inlet concentration of mercury was very low and difficult to control (e.g., 50 ± 20 $\mu g/N\,m^3$). In an attempt to closely monitor system operation, tests at representative conditions for selected flue gas compositions were completed with the FGD activated carbon. Linear correlations between equilibrium Hg^0 and $HgCl_2$ adsorption capacities and inlet concentrations were obtained with 83 and 104 data points, respectively. Differences in equilibrium Hg^0 adsorption capacities, at 50 $\mu g/N\,m^3$ inlet concentration, are statistically significant if the Hg^0 capacities are at least ±49% different from one another. For $HgCl_2$, the differences in $HgCl_2$ adsorption capacities are statistically significant if the $HgCl_2$ capacities are at least ±28% different from one another. These analyses were performed at a 95% confidence level.

Results and Discussion

Physical and Chemical Characteristics of Raw and Sulfur-Impregnated Adsorbents

In general, sulfur impregnation at 300 and 400°C resulted in an increase in total sulfur content and a decrease in total/micropore surface area and pore volume when compared to the raw samples (Table 1). As previously mentioned, a 0.02:1 to 0.05:1 sulfur to adsorbent mass ratio was used when impregnating sulfur into the fly ash and PSC samples. The mass ratios of total sulfur to PSC adsorbent were between 0.02 (2.1 wt %) and 0.04 (3.6 wt %), indicating that most of the added sulfur remained in the samples.

A 1:1 sulfur to adsorbent mass ratio was used when impregnating sulfur into the remaining CDAC, PAC, and zeolite samples. It was assumed that all of the samples treated with a 1:1 sulfur to adsorbent mass ratio were saturated with respect to their sulfur content at the specified experimental condition. Saturation of sulfur in carbon materials using sulfur impregnation at elevated temperatures was reported between 5 and 50 wt %, depending on the nature of the carbon, form of the sulfur reagent, and the experimental conditions (Bansal et al. 1988). The approach used in this study resulted in sulfur contents increasing to 9.4–22.4 wt % (Table 1), corresponding to 8.5–22.4 wt % sulfur added. In a previous study, a 3:1 sulfur to adsorbent mass ratio was used when impregnating elemental sulfur onto the ACF samples (Hsi et al. 2001). The resulting sulfur-impregnated ACF sample (i.e., ACF-20-S400) contained 44 wt % sulfur (Table 1). Duplicate tests using 1:1 sulfur to adsorbent mass ratio to impregnate ACF samples showed that all of the chemical and physical properties listed in Table 1 were within 8% of each other when comparing the results for samples treated with 1:1 and 3:1 sulfur to adsorbent mass ratios. This result supports the hypothesis that sulfur impregnation using 1:1 sulfur to adsorbent mass ratio also saturates the ACF sample with sulfur. The six samples that were saturated with sulfur at this condition (i.e., CDAC, PAC, zeolite, and ACF) exhibited larger amounts of sulfur added with increasing total surface area and micropore surface area of the raw sample (Table 1, Fig. 1).

The amount of sulfur added to the impregnated samples correlated to the percent reduction in total surface area and the percent reduction in pore volume with correlation coefficients (R^2) $\leq$0.73 (Fig. 2). All samples provided in Table 1 are included in Fig. 2, except for the fly ash and zeolite A samples. The fly ash samples were not included in this correlation because the raw samples did not have any detectable micropore surface area with the N_2–BET adsorption test. Zeolite A was not included because the pore size was too small for the sulfur to enter the porous structure of the adsorbent. Sulfur impregnation resulted in the largest total sulfur content (44 wt %) for the ACF sample, which had the largest reduction in total surface area (95%) and pore volume (95%). These linear regressions of sulfur added to reduc-

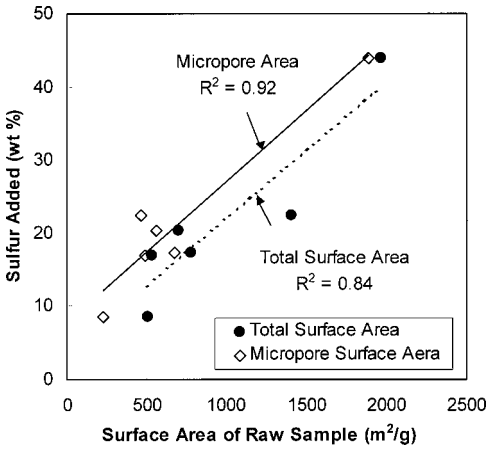

Fig. 1. Total surface area and micropore surface area of raw samples versus sulfur added for samples saturated with sulfur (coal derived activated carbons, pistachio activated carbon, zeolite Y, and activated carbon fiber-20).

tion in the surface area and pore volume suggest that the sulfur could be deposited onto the adsorbents by monolayer surface deposition or volume pore filling.

Pore size distributions of the adsorbents before and after sulfur impregnation indicate that pore widths are primarily between 5 and 10 Å (Fig. 3). A large portion (~51 mol %) of sulfur species in the gas phase at 400°C is S_2-S_6 (Tuller 1954). The diameters of S_2-S_6 were estimated to be between 5.2 and 6.9 Å on the basis of their molar volumes and assuming spherical sulfur molecules (*ChemSketch, 4.0*, 1999). The remaining gas-phase sulfur exists primarily as S_8 (49 mol %). The diameter of S_8 ranges from 7.6 to 8.4 Å depending on whether the molecule exists as a ring or a chain (ChemSketch 1999). Sulfur molecules that are smaller than the adsorbents' pore widths could penetrate inside many of the adsorbents' pores, adsorb onto the pore walls, fill the pores, or deposit onto the outer surface of the adsorbents. Sulfur molecules that are larger than the pores' widths can deposit on the outer surface and over the pores of the adsorbents. Therefore, reductions in surface area and pore volume as observed with the experimental results are consistent with the width of the samples' pores and the diameter of the gas-phase sulfur molecules studied here.

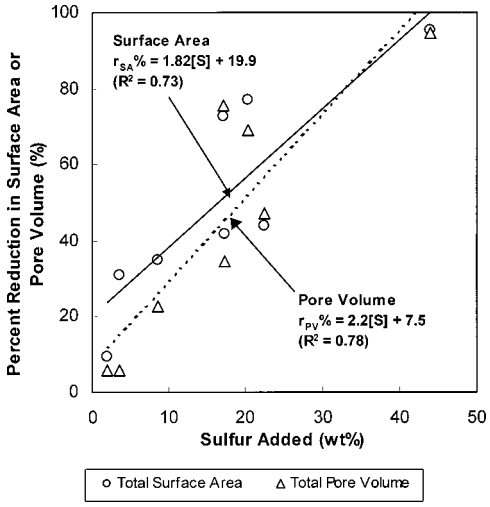

Fig. 2. Percent reduction in (♦) total surface area and (▲) pore volume with increasing sulfur added due to sulfur impregnation. r_{SA} and r_{PV} are reductions in surface area and pore volume, respectively. Data include coal derived activated carbons, pistachio shell chars, pistachio activated carbon, zeolite Y, and activated carbon fiber-20.

The same observations about monolayer surface deposition or volume pore filling can also be made by comparing calculated sulfur added for complete monolayer surface coverage and complete volume pore filling of samples to the measured amount of sulfur added due to sulfur impregnation (Fig. 4). These results were obtained using the surface areas and pore volumes based on the normalized 3D pore size distributions and the physical properties of samples shown in Table 1. No sulfur was assumed to be deposited into pores with widths less than the diameters of each of the gaseous sulfur molecules. For zeolite Y, cylindrical pore structure was assumed. Uniform distribution of elemental sulfur molecules in all pores with sufficient width was assumed. Results indicate that the mesoporous samples (i.e., FGD sample at 8.5 wt % sulfur added and FG3 sample at 22.4 wt % sulfur added) did not achieve complete monolayer surface coverage or pore filling with sulfur [Fig. 4(a)]. However, assuming the sulfur molecules were only deposited into the micropores of the samples results in all of the samples achieving complete monolayer surface coverage or volume filled pores with the sulfur, depending on the form of sulfur that was deposited onto the adsorbents [i.e., S_2-S_8, Fig. 4(b)]. These results suggest that sulfur molecules preferentially enter into the samples' micropores under the experimental conditions tested here.

Comparing the changes in micropore/mesopore surface areas and volumes as a result of sulfur impregnation allows further characterization of where the sulfur is deposited onto the adsorbents. Both the micropore surface area and volume of the primarily microporous PILOT-5 sample decreased by 87% after sulfur impregnation (Table 1). The PILOT-5 sample's mesopore surface area and volume both decreased by 33%. The PAC, zeolite, and ACF samples, which are also primarily microporous, also demonstrated much larger reductions in micropore surface area/volume compared to the reductions in mesopore surface area/volume. The mean and standard deviation of the percent reductions in micropore surface area and volume for PILOT-5, PAC, zeolite, and ACF samples were 77±20%. The mean and standard deviation of the percent reductions in mesoporous surface area and volume for the same samples were 35±31%. These standard deviations are so large compared to their corresponding mean values as to be meaningless. In contrast, FGD and FG3, which are primarily mesoporous activated carbons, had more uniform percent reductions in the micropore and mesopore surface area/volume (i.e., 38±4% and 37±13%, respectively). The reason(s) for such partitioning of the sulfur is not understood at this time.

Sulfate was the dominant sulfur species for the impregnated fly ash sample (53% of the total sulfur) while elemental sulfur constituted 40% of the total sulfur, and organic sulfur consisted of the sulfur balance as determined by S-XANES (Fig. 5). These results suggest that the impregnated sulfur reacts with the mineral compounds in the fly ash to form sulfate or remains as elemental sulfur. In contrast to the results for fly ash, elemental sulfur was the dominant sulfur form (78–95% of the total sulfur) for the remaining carbonaceous and zeolite samples. A portion of the elemental sulfur also reacted with the carbon adsorbents to form organic sulfur (6–12% of the total sulfur). The impregnated zeo-

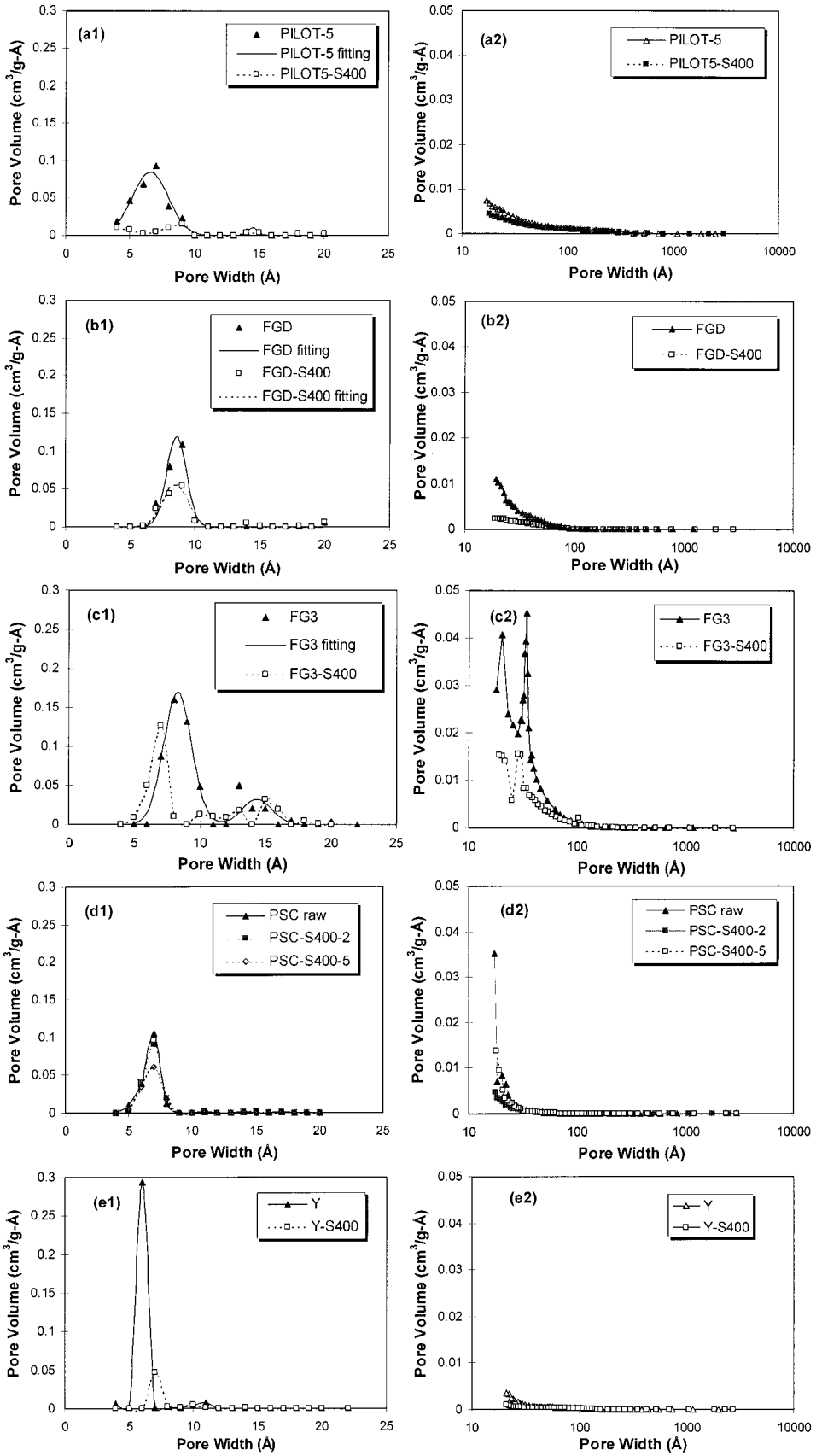

Fig. 3. (1) Micropore and (2) mesopore size distributions of raw and sulfur-impregnated samples (a)–(c) coal-derived activated carbon (PILOT-5, FGD, and FG3 samples, respectively), (d) biomass activated carbons (pistachio shell char samples), and (e) zeolite Y. Symbols on micropore size distributions are original data points obtained by 3D model. Select lines are made by fitting Gaussian curves to data for comparison.

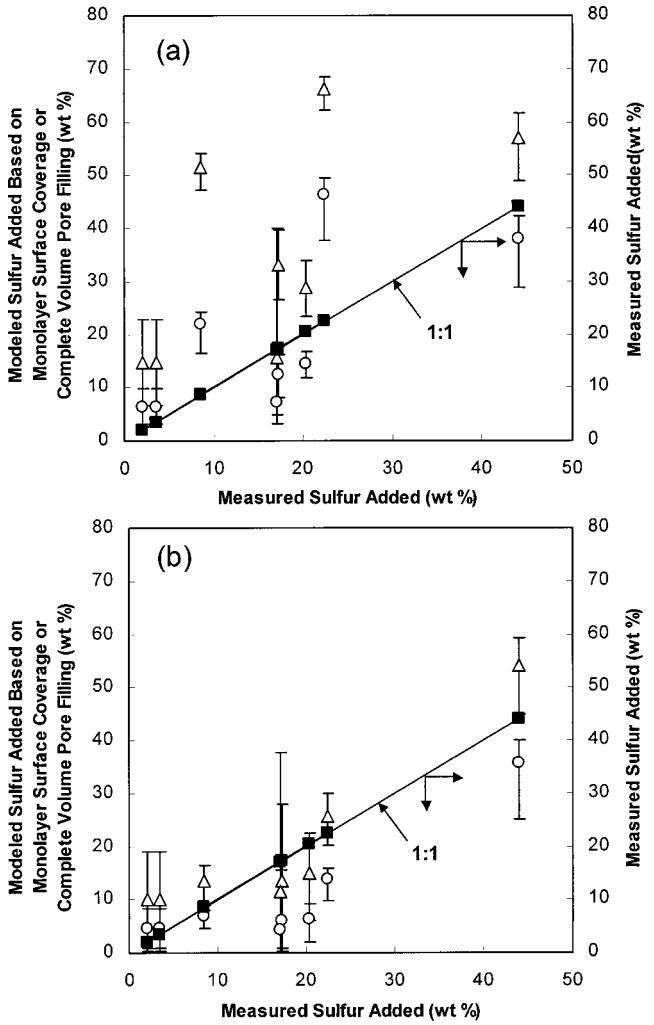

Fig. 4. Modeled sulfur added based on (○) complete monolayer surface coverage and (△) complete volume pore filling plotted versus (■) measured sulfur added for (a) total surface area and pore volume and (b) micropore surface area and volume. Vertical bars indicate ranges of modeled sulfur added for sulfur forms from S_2 to S_8. Data include coal derived activated carbons, pistachio activated carbon, zeolite, and activated carbon fibers but excluding fly ash samples and zeolite A.

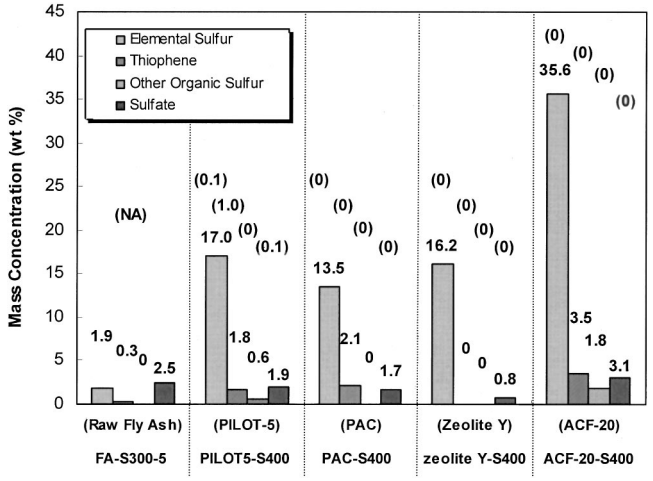

Fig. 5. Mass concentrations of sulfur functional groups for raw and sulfur-impregnated samples. Sample names and corresponding concentrations of sulfur functional groups [e.g., (0), (0.1), or (1.0)] for raw samples are presented in parentheses. (NA=not available.)

lite does not contain organic sulfur because these samples do not contain carbon to react with impregnated sulfur.

X-ray diffraction analyses were also completed on the pure crystalline elemental sulfur that was used to impregnate the samples, and on the sulfur that was impregnated in the zeolite (Y-S400), CDAC (PILOT5-S400), and ACF (ACF-20-S400). The pure sulfur sample and the sulfur in the zeolite were orthorhombic crystals. In contrast, the sulfur in the carbonaceous adsorbents was amorphous (i.e., no crystalline sulfur was detected). It is unclear at this time why the forms of elemental sulfur are different and whether the forms of elemental sulfur could result in different mercury adsorption capacities.

Mercury Adsorption Capacities

In general, the mercury adsorption capacities of raw samples containing ≥1.0 wt % sulfur (e.g., PILOT-5 and FGD) were at least 1.6 times larger than those for samples containing no detectable sulfur (except for the $HgCl_2$ adsorption of ACF-20 sample) (Table 1). Sulfur impregnation at 300 and 400°C increased both the equilibrium Hg^0 and $HgCl_2$ adsorption capacities compared to the corresponding samples without sulfur impregnation for the conditions tested here. All of the samples with detectable micropore surface area had equilibrium Hg^0 and $HgCl_2$ adsorption capacities from 89 to 3,260 and from 236 to 4,509 μg/g, respectively. The raw and sulfur-impregnated fly ash samples contained no detectable microporous structure while achieving equilibrium Hg^0 and $HgCl_2$ adsorption capacities up to 38 and 104 μg/g, respectively. These equilibrium Hg^0 and $HgCl_2$ adsorption capacities were 13 and 6 times smaller, respectively, than those for the impregnated PSC samples (up to 492 and 645 μg/g equilibrium Hg^0 and $HgCl_2$ adsorption capacities, respectively), which had comparable total sulfur contents (2.1–3.6 wt %) but larger micropore surface areas (300 ± 50 m^2/g). These results indicate that the adsorbents' porous structure, mainly as micropores for most of the carbonaceous samples in this study, is one of the important factors for Hg^0 and $HgCl_2$ adsorption. These results further support the fact that materials with sufficient amounts of active adsorption sites (e.g., sulfur) and sufficient microporous structure are needed to achieve large mercury adsorption capacities (Hsi et al. 2001).

The raw zeolite A and Y samples had small equilibrium Hg^0 and $HgCl_2$ adsorption capacities that were between 0 and 236 μg/g. These results were anticipated because raw zeolites were not expected to contain active adsorption sites for mercury. After sulfur impregnation at 400°C, the sulfur contents of these noncarbonaceous samples increased from 0 to 12–17 wt %, which were comparable to impregnated CDACs and PACs (total sulfur content=9.4–22.4 wt %) (Table 1). However, sulfur-impregnated zeolites had much smaller equilibrium Hg^0 and $HgCl_2$ adsorption capacities (0–236 μg/g), which were at least six times smaller than those for the sulfur-impregnated CDAC (sample PILOT5-S400), and at least four times smaller than that for sulfur-impregnated PAC (sample PAC-S400) (Table 1). Zeolite A had micropores with a small pore width (3.5 or 3.9 Å), which is smaller than the diameter of the mercury compounds tested here. These relative dimensions contributed to the small equilibrium mercury adsorption capacities. However, comparison of the properties of sulfur-impregnated zeolite Y (Y-S400) to coal-based

PILOT5-S400 indicates that their elemental sulfur contents (16.2 versus 17.0 wt %), total surface areas (146 versus 160 m^2/g), micropore surface areas (112 versus 72 m^2/g), and pore size distributions (with a 7 Å peak modeled by the 3D method) were very similar. The equilibrium Hg^0 adsorption capacities for these two samples, however, were 11 times different (Table 1).

Results provided above suggest that sulfur-impregnated zeolites had small mercury adsorption capacities because: (1) the forms of elemental sulfur play different roles in mercury adsorption (e.g., S_2 versus S_8 and/or amorphous versus crystalline sulfur); (2) the organic sulfur content of the sites on the carbonaceous adsorbent are important for mercury adsorption (Hsi et al. 1998); and/or (3) the shape of the micropores (slit pores versus cylindrical pores for activated carbon and zeolite, respectively) may influence mercury adsorption capacities. It is also important to note that zeolite samples used in this study are highly hydrophilic. These zeolite samples were stored in air, typically contained 15–20 wt % H_2O (including adsorbed and crystal H_2O), and were not dehydrated before the bench-scale mercury adsorption tests. The adsorbed H_2O, which was expected in the micropores of zeolites, may inhibit the access of mercury into the microporous structure (Liu et al. 2000).

Linear correlations between total sulfur content and equilibrium Hg^0 and $HgCl_2$ adsorption capacities are shown in Fig. 6 for all data provided in Table 1. Linear correlations between mercury adsorption capacities and total sulfur content were insignificant ($R^2=0.02$ for both Hg^0 and $HgCl_2$ adsorption) for samples with sulfur contents <5 wt %. Such a result indicates that sulfur contents <5 wt % were not the controlling factor, especially when compared to more thoroughly analyzed results that are provided below. At this range of sulfur content, the equilibrium Hg^0 and $HgCl_2$ adsorption capacities were between 0 and 1,000 μg/g. However, when the 400°C sulfur-impregnated samples with sulfur contents >5 wt % were included in the regression, there was an increase in the R^2 values to 0.73 and 0.74 for equilibrium Hg^0 and $HgCl_2$ adsorption capacities, respectively. The intercepts at the ordinate that were obtained from the linear regressions of Hg^0 and $HgCl_2$ adsorption capacities to sulfur content were 115.8 and 221.9 μg/g, respectively, which indicated the equilibrium Hg^0 and $HgCl_2$ adsorption capacities for adsorbents without any sulfur. These intercept values were, in general, smaller than the equilibrium Hg^0 and $HgCl_2$ adsorption capacities for raw carbonaceous adsorbents without sulfur (e.g., PAC and ACF). This result may be due to the contribution of micropores without sulfur active sites and/or oxygenated functional groups on the carbonaceous adsorbents to the samples' mercury adsorption capacities (Matsumura 1974). The equilibrium Hg^0 and $HgCl_2$ adsorption capacities for all of the 400°C sulfur-impregnated carbonaceous adsorbents with sulfur contents >5 wt % were between 393 and 4,509 μg/g.

The R^2 values relating total sulfur contents and equilibrium Hg^0 and $HgCl_2$ adsorption capacities increased to 0.86 and 0.82, respectively, for the carbonaceous adsorbents (i.e., zeolite samples were excluded). The increase in the R^2 values is due to the removal of samples (i.e., zeolites) that are influenced by other factors as described above. The slopes of the linear regressions for the carbonaceous adsorbents were 59.2 and 96.8 μg Hg/wt % S for Hg^0 and $HgCl_2$, respectively; indicating that 1 mol S captures 0.001 mol Hg^0 and 0.0016 mol $HgCl_2$ (as Hg) in the simulated coal-combustion flue gases. These results indicate that for the carbonaceous samples tested here, mercury in the adsorbed phase is linearly dependent on the total sulfur content of the adsorbents at this small concentration (50 ± 20 μg/N m^3) of gas-phase mercury.

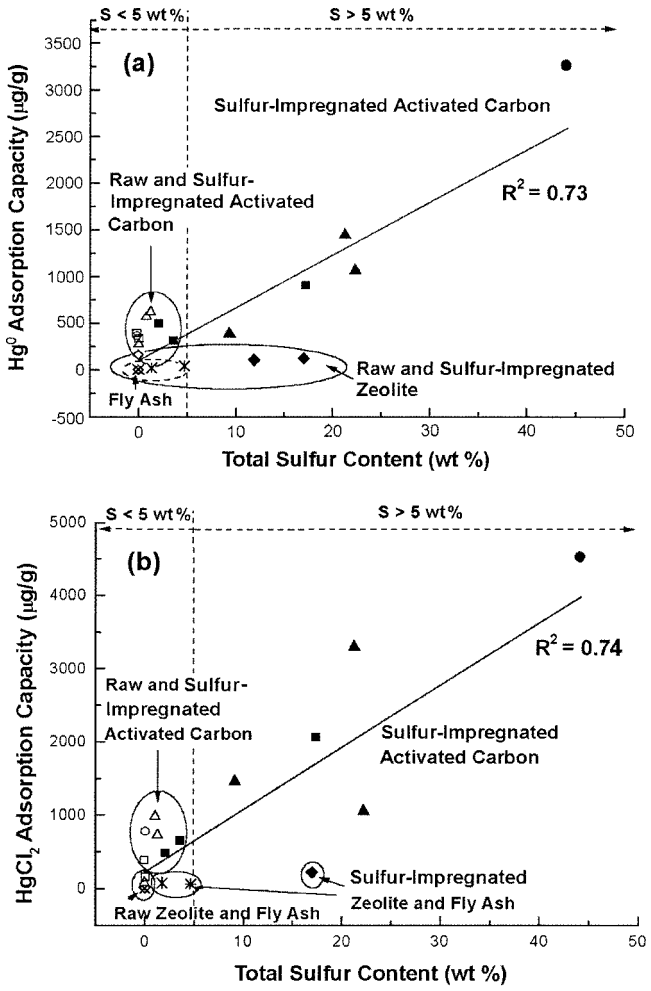

Fig. 6. (a) Hg^0 and (b) $HgCl_2$ adsorption capacity dependence of total sulfur content: (×) raw fly ash, (∗) sulfur-impregnated fly ash, (△) raw coal derived activated carbons, (▲) sulfur-impregnated coal derived activated carbons, (□) raw pistachio shell chars and pistachio activated carbon, (■) sulfur-impregnated pistachio shell chars and pistachio activated carbon, (◇) raw zeolites, (◆) sulfur-impregnated zeolites, (○) raw activated carbon fibers, and (●) sulfur-impregnated activated carbon fibers. R^2 values of 0.73 and 0.74 were obtained using all of samples provided in Table 1.

Multiple regressions were performed (SPSS®, Version 10.0) for the carbonaceous adsorbents that were analyzed for their sulfur forms to further understand the effects of sulfur forms on mercury adsorption capacities (Table 2). The data set (ten data points) included FA-S300-5, PILOT-5, PILOT5-S400, PAC, PAC-S400, ACF-20, and ACF-20-S400 samples described in Fig. 5, and those samples with very low sulfur contents that are assumed to be zero (i.e., raw fly ash, FG3, and PSC). Sulfate was excluded from the analyses because no linear relationship ($R^2\leqslant0.48$) can be established between its quantity and mercury adsorption capacities. Results showed that linear correlations were established between equilibrium Hg^0 and $HgCl_2$ adsorption capacities and the independent variables, elemental sulfur, and organic sulfur contents ($R^2=0.94$ and 0.92, respectively). These correlations also showed that without any elemental and organic sulfur, the Hg^0 and $HgCl_2$ adsorption capacities were 165.1 and 304.9 μg/g, re-

Table 2. Multiple Linear Regressions for Mercury Adsorption Capacities as They Depend on Sulfur Functional Group Content for Raw and Sulfur-Impregnated Carbonaceous Samples

	Variable	Coefficients	Standard error	R^2
Hg^0[a]	Constant	165.1	98.6	0.94
	Elemental sulfur	19.7	38.9	
	Organic sulfur	415.7	267.7	
$HgCl_2$[b]				
	Constant	304.9	181.1	0.92
	Elemental sulfur	83.6	71.5	
	Organic sulfur	301.1	491.6	

[a]Hg^0 adsorption capacity=165.1±(98.6)+(19.7±38.9)[elemental S]+(415.7±267.7)[organic S].

[b]$HgCl_2$ adsorption capacity=304.9±(181.1)+(83.6±71.5)[elemental S]+(301.1±491.6)[organic S].

spectively. These capacities were comparable to those obtained from linear regression shown in Fig. 6 (115.8 and 221.9 μg/g, respectively). Increasing the elemental and organic sulfur contents increased the mercury adsorption capacities, suggesting that both elemental and organic sulfur are important active sites for Hg^0 and $HgCl_2$ adsorption.

The dependencies of Hg^0 and $HgCl_2$ adsorption capacities on total surface area are shown in Fig. 7. The R^2 values for mercury adsorption capacity to total surface area were <0.02, indicating that total surface area and mercury adsorption capacities are not correlated for the conditions tested here [Figs. 7(a and b)]. However, it is important to mention again that samples without detectable sulfur content and with a negligible surface area (such as fly ash) had the smallest Hg^0 and $HgCl_2$ adsorption capacities, indicating the importance of active sulfur sites and porous structure for mercury adsorption. When the equilibrium Hg^0 and $HgCl_2$ adsorption capacities were correlated to total surface area [Figs. 7(c and d)] for sulfur-containing samples with 0.1–5.0 wt % sulfur content, the R^2 values increased to 0.97 and 0.66, respectively. Those low-sulfur samples did not provide significant correlations ($R^2<0.14$) between mercury adsorption capacities and total sulfur content (Fig. 6).

The equilibrium Hg^0 adsorption capacities for all samples with 0.1–5.0 wt % sulfur content can also be correlated to micropore surface area ($R^2=0.80$) but not mesopore area ($R^2=0.50$), indicating the importance of micropores for Hg^0 adsorption when active sulfur sites are available. The equilibrium $HgCl_2$ adsorption capacities for the same samples can neither be correlated to micropore surface area ($R^2=0.40$) nor to mesopore area ($R^2=0.68$), indicating the difference in adsorption mechanisms between Hg^0 and $HgCl_2$. These trends between physical properties and mercury adsorption capacities were consistent with a previous study on a series of high- and low-sulfur CDACs, which contain sulfur between 0.8 and 2.6 wt % (Hsi et al. 1998).

Summary and Conclusions

This study described the influence of sulfur impregnation at 300 and 400°C on the chemical and physical properties of carbonaceous and noncarbonaceous adsorbents, and the relationships between those properties and the samples' equilibrium Hg^0 and $HgCl_2$ adsorption capacities in simulated coal-combustion flue gas conditions. In general, sulfur impregnation increased the total sulfur content and decreased the total/micropore surface area and

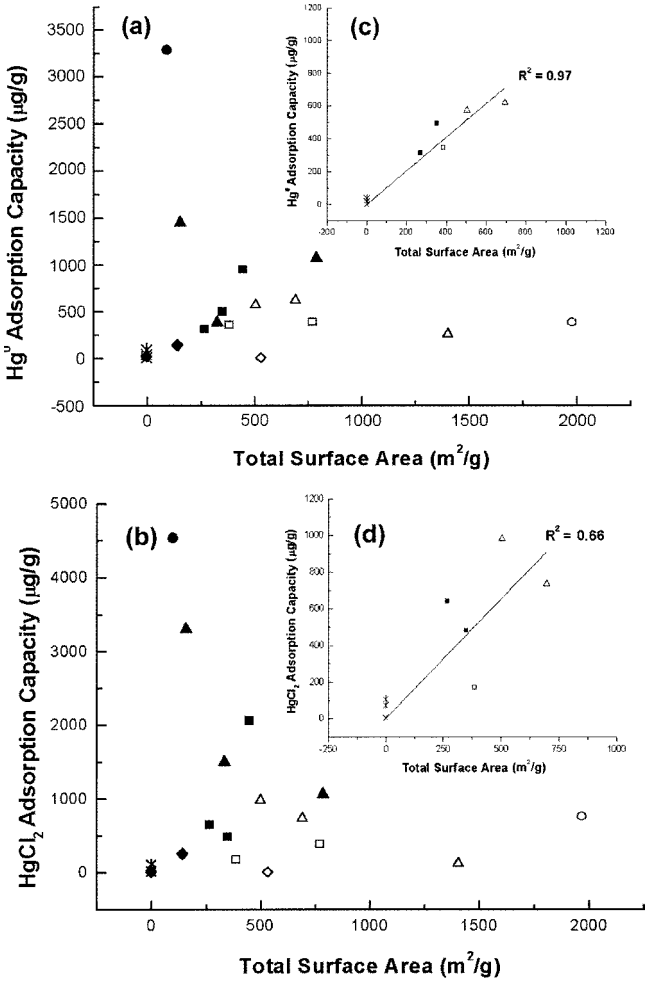

Fig. 7. (a) Hg^0 and (b) $HgCl_2$ adsorption capacity dependence of total surface area: (×) raw fly ash, (∗) sulfur-impregnated fly ash, (△) raw coal derived activated carbons, (▲) sulfur-impregnated coal derived activated carbons, raw pistachio shell chars and pistachio activated carbon, (■) sulfur-impregnated pistachio shell chars and pistachio activated carbon, (◇) raw zeolites, (◆) sulfur-impregnated zeolites, (○) raw activated carbon fibers, and (●) sulfur-impregnated activated carbon fibers (□). Data sets are from Table 1 with sulfur contents between 0.1 and 5 wt % as shown in (c) for Hg^0 adsorption capacities and (d) for $HgCl_2$ adsorption capacities.

pore volume of all samples tested. Elemental sulfur, organic sulfur, and sulfate formed after sulfur impregnation. This is the first study that has demonstrated that fly ash, CDAC, PSC, PAC, zeolite, and ACF (using coal-based, biomass, phenolic-based, and aluminosilicate precursors) exhibit the same trends in surface area and pore volume. The resulting total sulfur contents were correlated to the samples' initial physical properties, such as total surface area and pore volume, indicating that sulfur could be introduced onto the adsorbents by monolayer surface deposition or volume pore filling.

The chemical and physical properties of adsorbents played important roles in Hg^0 and $HgCl_2$ adsorption. In general, sulfur impregnation improved mercury adsorption. The equilibrium Hg^0 and $HgCl_2$ adsorption capacities were correlated to the total sulfur content of carbonaceous adsorbents ($R^2=0.86$ and 0.82, respectively) for the wide range of carbonaceous adsorbents studied here. Results showed that no significant correlation could be made between the mass concentrations of sulfate and the equilib-

rium $Hg^0/HgCl_2$ adsorption capacities. Correlations with $R^2 \geq 0.92$ were established between the equilibrium $Hg^0/HgCl_2$ adsorption capacities and the mass concentrations of elemental and organic sulfur. These results indicate that elemental and organic sulfur are active adsorption sites for Hg^0 and $HgCl_2$.

The equilibrium Hg^0 adsorption capacities for carbonaceous adsorbents containing 0.1–5.0 wt % sulfur were correlated to their total and micropore surface area ($R^2 = 0.80–0.97$), indicating that Hg^0 adsorption was dependent on the physical characteristics, especially micropores when active sulfur sites were available, in this sulfur content range. Correlations could not be made between equilibrium $HgCl_2$ adsorption capacities and total or micropore surface areas ($R^2 \leq 0.66$) for the sample sulfur content range, revealing the difference in adsorption behaviors for Hg^0 and $HgCl_2$.

To achieve sufficiently large equilibrium mercury adsorption capacities (i.e., $\geq$1,000 μg/g), suitable chemical (sulfur content >5 wt %) *and* physical properties (micropore area ≥ 70 m^2/g) are needed. Sulfur-impregnated zeolites had small mercury adsorption capacities, which may be due to the difference between carbonaceous and noncarbonaceous adsorbents in terms of the forms of sulfur, sizes, and shapes of the micropores, and H_2O contents. Further studies are needed to gain a better understanding of adsorption of mercury on zeolite adsorbents.

Acknowledgments

Funding support from the EPRI (Grant No. WO8303-02) is appreciated. The writers acknowledge Dr. Carl Richardson (URS Corp.) for the mercury adsorption tests, Dr. Frank Huggins (University of Kentucky) for S-XANES examinations, and Dr. Dewey Moore (Illinois State Geological Survey) for XRD examinations.

References

Adriano, D. C., Page, A. L., Elseewi, A. A., Chang, A. C., and Staughan, I. (1980). ''Utilization and disposal of fly ash and other coal residues in terrestrial ecosystems: A review.'' *J. Environ. Qual.*, 9(3), 333–344.

ASTM. (1997a). ''Standard test methods for carbon black-surface area by multipoint B.E.T. nitrogen adsorption.'' *D4820-96a*, West Conshohocken, Pa.

ASTM. (1997b). ''Standard test methods for sulfur in the analysis sample of coal and coke using high temperature tube furnace combustion methods.'' *D4239-94*, West Conshohocken, Pa.

Bansal, R. C., Donnet, J.-B., and Stoeckli, F. (1988). *Active carbon*, Marcel Dekker, New York.

Breck, D. W. (1973). *Zeolite molecular sieves*, Wiley, New York.

Carey, T. R., Hargrove, O. W., Jr., Richardson, C. F., Chang, R., and Meserole, F. B. (1998). ''Factors affecting mercury control in utility flue gas using activated carbon.'' *J. Air Waste Manage Assoc.*, 48, 1166–1174.

Chang, R., and Offen, G. R. (1995). ''Mercury emission control technologies: An EPRI synopsis.'' *Power Eng.*, November, 51–57.

Gregg, S. J., and Sing, K. S. W. (1967). *Adsorption, surface area and porosity*, Academic, New York.

Hsi, H.-C., Chen, S., Rostam-Abadi, M., Rood, M. J., Richardson, C. F., Carey, T. R., and Chang, R. (1998). ''Preparation and evaluation of coal-derived activated carbons for removal of mercury vapor from simulated coal combustion flue gases.'' *Energy Fuels*, 12(6), 1061–1070.

Hsi, H.-C., Rood, M. J., Rostam-Abadi, M., Chen, S., and Chang, R. (2001). ''Effects of sulfur impregnation temperature on the properties and mercury adsorption capacities of activated carbon fibers (ACFs).'' *Environ. Sci. Technol.*, 35(13), 2785–2791.

Huggins, F. E., Vaidya, S. V., Shah, N., and Huffman, G. P. (1993). ''Investigation of sulfur forms extracted from coal by perchloroethylene.'' *Fuel Process. Technol.*, 35, 233–257.

Kerr, G. T. (1966). ''Chemistry of crystalline aluminosilicates. I. Factors affecting the formation of zeolite A.'' *J. Phys. Chem.*, 70(4), 1047–1049.

Korpiel, J. A., and Vidic, R. D. (1997). ''Effect of sulfur impregnation method on activated carbon uptake of gas-phase mercury.'' *Environ. Sci. Technol.*, 31(8), 2319–2325.

Krishnan, S. V., Gullett, B. K., and Jozewicz, W. (1994). ''Sorption of elemental mercury by activated carbons.'' *Environ. Sci. Technol.*, 28(8), 1506–1512.

Lippens, B. C., Linsen, B. G., and de Boer, J. H. (1964). ''Studies on pore systems in catalysts I. The adsorption of nitrogen; apparatus and calculation.'' *J. Catal.*, 3, 32–37.

Liu, W., Vidic, R. D., and Brown, T. D. (1998). ''Optimization of sulfur impregnation protocol for fixed-bed application of activated carbon-based sorbents for gas-phase mercury removal.'' *Environ. Sci. Technol.*, 32(4), 531–538.

Liu, W., Vidic, R. D., and Brown, T. D. (2000). ''Impact of flue gas conditions on mercury uptake by sulfur-impregnated activated carbon.'' *Environ. Sci. Technol.*, 34(1), 154–159.

Livengood, C. D., Huang, H. S., and Wu, J. M. (1994). ''Experimental evaluation of sorbents for the capture of mercury in flue gases.'' *Proc., 87th Annual Meeting and Exhibition of the Air and Waste Management Assoc.*, Cincinnati.

Matsumura, Y. (1974). ''Adsorption of mercury vapor on the surface of activated carbons modified by oxidation or iodization.'' *Atmos. Environ.*, 8, 1321–1327.

Steijns, M., Peppelenbos, A., and Mars, P. (1976). ''Mercury chemisorption by sulfur adsorbed in porous materials.'' *J. Colloid Interface Sci.*, 57(1), 181–186.

Sun, J., Chen, S., Rood, M. J., and Rostam-Abadi, M. (1998). ''Correlating N_2 and CH_4 adsorption on microporous carbon using a new analytical model.'' *Energy Fuels*, 12(6), 1071–1078.

Tuller, W. N., ed. (1954). *The sulphur data book*, McGraw-Hill, New York.

U.S. Environmental Protection Agency (USEPA). (1997). ''Mercury study report to congress volume VIII: An evaluation of mercury control technologies and costs.'' *Rep. No. EPA-452/R-97-005*, Office of Air Quality Planning and Standards and Office of Research and Development, Research Triangle Park, N.C.